Structural, transport, and magnetic properties of Ru1-xMxSr2GdCu2O8 (M = Ti and Rh for 0<x<0.2)

Arafa Hassen, Joachim Hemberger, Alois Loidl, Alexander Krimmel

Angaben zur Veröffentlichung / Publication details:

Hassen, Arafa, Joachim Hemberger, Alois Loidl, and Alexander Krimmel. 2002. "Structural, transport, and magnetic properties of Ru1-xMxSr2GdCu2O8 (M = Ti and Rh for 0<x<0.2)." *Physica. C* 400 (1-2): 71–80. https://doi.org/10.1016/S0921-4534(03)01330-3.

Structural, transport and magnetic properties of $Ru_{1-x}M_xSr_2GdCu_2O_8$ (M = Ti and Rh for $0 \leqslant x \leqslant 0.2$)

A. Hassen, J. Hemberger, A. Loidl, A. Krimmel *

Experimentalphysik V, Elektronische Korrelation und Magnetismus, Institut für Physik, Universität Augsburg, Universitaetsstrasse 1, 86135 Augsburg, Germany

1. Introduction

Since the discovery of ferromagnetism coexisting with superconductivity in rutheno-cuprates, many reports on $RuSr_2R_{2-x}Ce_xCu_2O_{10+\delta}$ (Ru-1222) and $RuSr_2RCu_2O_8$ (Ru-1212) where R is Gd, Eu or Y [1–12], have been given. These compounds were first synthesized by Bauerfeind et al. [13,14] and are the only high-T_c compounds where the magnetic ordering temperature is much higher than the superconducting transition. The Ru-1212 compounds contain Cu double layers with the Gd(Eu) sandwiched in between. The copper ions are in the basal plane of oxygen half pyramids, which are connected to ruthenium in an octahedral environment. Hence, in these rutheno-cuprates, the RuO_2 layers replace the CuO chains of the R123 high-T_c cuprates as charge reservoir. In the case of Ru^{5+} ($4d^3$, $S = 3/2$), the CuO_2 layers would be built up by Cu^{2+} and the Ru-1212 compounds would be insulators. Assuming hole doping of the copper planes, mixed valence behavior (Ru^{4+}/Ru^{5+}) of the ruthenium ions is the

* Corresponding author. Tel.: +49-821-5983606; fax: +49-821-5983649.

E-mail address: alexander.krimmel@physik.uni-augsburg.de (A. Krimmel).

direct consequence. Ru^{4+} corresponds to a $4d^4$ configuration yielding a spin $S = 1$ [15–17].

Neutron diffraction experiments [9,10] below T_N revealed a G-type antiferromagnetic (AFM) structure for the Ru sublattice, with an ordered moment of the order of 1 μ_B. The Gd ions order independently below 2.5 K also with a G-type spin configuration. Both diffraction studies put an upper limit of 0.1 μ_B [9] or 0.3 μ_B [10] to any net zero-field ferromagnetic (FM) moment. Later on, from low-field magnetization measurements on $RuSr_2EuCu_2O_8$ it has been concluded that the FM moment is of the order of 0.05 μ_B/Ru at 5 K [11].

The origin of the FM moment is still unclear. Of course, weak ferromagnetism can have its origin in the Dzyaloshinski–Moriya interaction. There is an ongoing dispute if the symmetry of the Ru-1212 compounds allows for a non-zero antisymmetric superexchange [9]. Another source of providing a canting of the Ru spins would be the double-exchange interaction. In principle, the mixed valence behavior of the RuO_2 planes makes such an interaction plausible, which is responsible for the occurrence of ferromagnetism in the Mn perovskites and dominates the phase diagram of $LaMnO_3$ at low doping levels where it gives rise to an insulating canted antiferromagnet [18]. And indeed, recently the double-exchange mechanism has been proposed to be responsible for the weak ferromagnetism in the rutheno-cuprates [19]. Finally, based on detailed NMR studies [16] the possibility of ferromagnetism in a charge-ordered state of the RuO_2 planes has been suggested.

The bulk superconductivity originates from the CuO_2 bilayers [12,21] and the Ru-1212 system behaves as a typical underdoped high-T_c superconductor [12,21]. Pickett et al. [7] pointed out that the layers carrying superconductivity and magnetism are thin enough to warrant the coexistence of the two properties in the same unit cell. This implies that the magnetic coupling perpendicular to the layers is weak enough to allow for superconductivity. There is no clear evidence that Ru-1212 exhibits a bulk Meissner state (MS) [22–24]. However, Bernhard et al. [12] reported that for $T < 30$ K and in external fields $H \leqslant 30$ Oe there is a sizable amount of diamagnetic signal corresponding to a MS. The possible existence of a self-induced vortex state has recently been put on firm grounds by NMR investigations of $RuSr_2YCu_2O_8$ [20].

The effect of doping on the physical properties of rutheno-cuprate systems has been investigated by several groups [22,25–27,29,33]. The superconducting and magnetic properties of Ru-1212 are strongly affected by the type of dopant and by the substitutional site. Focusing first on substitutional series at the Ru site, McLaughlin and Attfield [26] prepared $Ru_{1-x}Sn_xSr_2GdCu_2O_8$ and investigated the effect of Sn defects on superconductivity and ferromagnetism. They observed that Sn suppresses the ferromagnetic moment in the Ru layers and that the Néel temperature (T_N) decreases from 138 K in the pure compound to 78 K for $x = 0.4$. On the other hand, the superconducting transition temperature (T_c) is increased from 36 K in the undoped material ($x = 0$) to 42 K for $x = 0.2$. These results were attributed to the diamagnetic properties of the Sn ions that do not contribute to the magnetic properties and therefore the total magnetic moment in the RuO_2 layers is reduced. Furthermore, the enhancement of the superconductivity in Sn-doped compounds may reflect the fact that the hole density in the copper planes becomes increased. This result is different from observations in Nb-doped compounds [34] in which the substitution of Ru by Nb decreases both T_N and T_c. Also the variation of the room-temperature Seebeck coefficient on Nb or Sn doping is different. Most probably the number of holes is increased for Sn, but decreased for Nb doping. Similarly, the magnetic and superconducting properties of $Ru_{1-x}M_xSr_2GdCu_2O_8$, with M = Ti, V and Nb for $x = 0.10$ and 0.20, have been investigated by Rijssenbeek et al. [27] and Malo et al. [29]. It was noticed that the solubility range of these cations depends on their oxidation states and ionic radius. Because of the limited solubility of Ti, impurity peaks in the X-ray diffraction data due to the formation $RuSrO_3$ showed up [29]. Both T_c and T_N are strongly affected by doping and were found to decrease for Ti and Nb, but are enhanced for V. The superconductivity was fully suppressed for Ti concentrations $x \geqslant 0.1$.

This behavior differs strongly from doping at the Cu or Sr site, respectively. E.g. substituting 3% Zn for Cu is sufficient to suppress superconductivity

due to pair breaking [30]. The extreme sensitivity of superconductivity towards Zn doping is well known from other high-T_c materials and has been studied in detail for the YBCO and LSCO systems [31,32]. Moreover, the superconducting state of Ru-1212 is also very susceptible to defects at the Sr site. Superconductivity is suppressed as well by substituting 3% La for Sr but due to a different mechanism: here the charge carriers in the CuO_2 planes are strongly reduced due to an efficient defect trapping [33].

Electron doping can be achieved by substituting Ce^{4+} for Gd^{3+} and it has been shown that in this case T_c is lowered while the AFM transition temperature is increased [35]. The successful synthesis of $Ru_{1-x}Sr_2GdCu_{2+x}O_8$ has been reported by Klamut et al. [22]. When Cu is substituted for Ru the superconducting phase transition is strongly enhanced, reaching values close to 70 K for $x = 0.7$. At the same time, long-range magnetic order is strongly suppressed and T_N is shifted well below the superconducting transition temperature.

We think it is worthwhile to perform further detailed and systematic doping experiments to elucidate the magnetic properties of the rutheno-cuprates. Substitutional defects, depending on their spin value, should enhance or decrease the magnetic ordering transition. Especially, the valence and spin state of the dopants should give some hints on the origin and nature of the ferromagnetic moment in Ru-1212. In addition, the substitution of Ru by non-isoelectronic defects also changes the charge reservoir and hence may also influence the superconducting properties. Substituting Ti^{4+} ($3d^0$) for ruthenium will slightly increase the hole doping and, as a consequence, should slightly increase T_c. But certainly the replacement of Ru by an ion with an empty d-shell will weaken the magnetic interaction and we expect a significant reduction of T_N. Concerning the effects of rhodium substitution we expect a similar increase of the hole doping: in oxides the valency of Rh is 3+ or 4+ and we expect that the most stable configuration Rh^{3+} will replace Ru^{4+}/Ru^{5+}. Concerning the magnetic properties, in an octahedral environment Rh^{3+} ($4d^6$) constitutes a non-magnetic $S = 0$ state and we expect a similar reduction of T_N as for Ti doping.

2. Experimental

Both pure and doped samples were prepared by employing conventional solid sate reactions [14]. Stoichiometric amounts of high purity powders of RuO_2, $SrCO_3$, Gd_2O_3, CuO, TiO_2 and Rh_2O_3 were used. After drying Gd_2O_3 at 1000 °C for 15 h, the powders were mixed in an appropriate ratio and calcinated at 930 °C in air. The products of the pure ($RuSr_2GdCu_2O_8$) and doped ($Ru_{1-x}M_xSr_2GdCu_2O_8$ where M = Ti and Rh for $0 \leqslant x \leqslant 0.2$) compounds were ground, pressed into pellets and heated for 12 h at 1020 °C in nitrogen [14] or pure argon [25] respectively to reduce the parasitic $RuSrO_3$ phase. The pellets were then reground into fine powders and put into a furnace at 1040 °C for 12 h in oxygen flow, followed by slow cooling. The sintering process was repeated twice at temperatures of 1050 and 1055 °C with intermediate grindings. Finally the samples were again pressed into pellets and annealed for six days at 1060 °C in oxygen and cooled slowly to room temperature with a rate of 30 °C/h.

All samples were characterized by X-ray powder diffraction with a Stoe X-ray diffractometer using the Cu-K_α radiation ($\lambda = 1.5406$ Å). The measurements were performed at room temperature for $20° \leqslant 2\theta \leqslant 80°$ with steps of 0.02°. The X-ray data were analyzed by standard Rietveld refinement. From these powder X-ray diffraction measurements we infer a better sample quality of the doped compounds for a heat treatment in pure argon. Therefore, the following results refer to these samples only. The measurements of DC magnetic susceptibilities were performed employing a Quantum Design SQUID. The DC resistivity was determined in the temperature range 2 K $< T <$ 300 K by a standard four-probe method.

3. Results and discussion

3.1. Crystal structure

The X-ray diffraction patterns of some representative doped compounds of $Ru_{1-x}M_xSr_2GdCu_2O_8$ with M = Ti and Rh are shown in Fig. 1. For low doping levels ($x \leqslant 0.05$ for M = Ti and

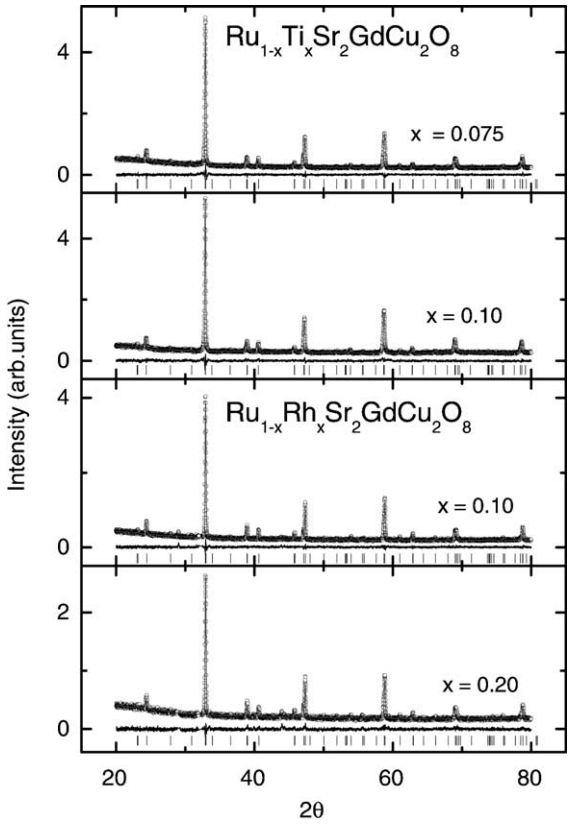

Fig. 1. Room temperature X-ray diffraction pattern of $Ru_{1-x}M_xSr_2GdCu_2O_8$, where M is Ti ($x = 0.075$ and 0.1) and Rh ($x = 0.1$ and 0.2) employing Cu-K_α radiation ($\lambda = 1.5406$ Å). The vertical bars of each diagram denote the peak positions due to space group *P4/mmm*. The results of the Rietveld analysis are indicated as solid lines. The difference patterns are indicated at the bottom of each pattern.

$x \leqslant 0.10$ for M = Rh, respectively) all investigated compounds are single phase. For a few compounds at high doping concentrations, weak additional intensities are observed close to $2\theta = 31.5°$ or $2\theta = 44°$ (see lower panel of Fig. 1). For M = Ti, the emergence of secondary phases at high doping concentrations has been attributed to the limited solubility of Ti ions [29]. Based on the X-ray diffraction data alone it is not possible to unambiguously identify the spurious phases. In the literature, these additional reflection are attributed to residual amounts of either $RuSrO_3$ [13] or Gd_2CuO_4 [36,37]. These compounds reveal magnetic order around 165 and 260 K, respectively. $RuSrO_3$ is a robust itinerant ferromagnet and it has been shown in detail that admixtures of $SrRuO_3$ to Ru-1212 induce pronounced changes of its magnetic behavior [39]. However, we found no anomalies in the magnetic measurements close to these temperatures, indicating that the amount of spurious phases is marginal.

All investigated compounds exhibit tetragonal symmetry described by space group *P4/mmm* with atoms located at Wyckoff positions (1b)$(0, 0, 1/2)$ for Ru, Ti or Rh, (2h)$(1/2, 1/2, z)$ for Sr, (1c)$(1/2, 1/2, 0)$ for Gd, (2g)$(0, 0, z)$ for Cu, whereas oxygen ions are distributed among the (8s)$(x, 0, z)$, (4i)$(0, 1/2, z)$ and (4o)$(x, 1/2, 1/2)$ positions, respectively. The results of the refinements of the X-ray diffraction patterns of Ti and Rh samples are summarized in Tables 1 and 2, respectively. No significant difference of the bond angle ϕ is detected for the Rh- and Ti-doped compounds, despite the different atomic size of these cations. The crystallographic structure is closely related to that of other 1212-type cuprate superconductors. The RuO_6-octahedra are connected via their apical oxygen ions with the CuO_5 square pyramids. The Cu–O–Ru bond angle, which characterizes the distortion of the RuO_6-octahedra, is essential for both the magnetic exchange interaction and the charge transfer between Ru–O and Cu–O layers. The changes in the lattice parameters, as well as the Cu–O–Ru bond angle are marginal within the investigated concentration range of Ti and Rh doping.

3.2. DC resistivity

The normalized resistivity values of all investigated compounds are shown in Fig. 2 (Ti-doping: upper frame; Rh-doping: lower frame). Due to microcracks in the ceramic samples, the absolute values of resistivities may not be very reliable and the room-temperature normalization is used to reveal the different temperature dependencies of the resistivity of the different samples. The pure compound is included in both frames for comparison with the doped samples. For both series, the resistivity increases with increasing doping. The doped samples reveal superconductivity until $x = 0.075$ for Ti and $x = 0.15$ for Rh-doping,

Table 1
Crystallographic properties of $Ru_{1-x}Ti_xSr_2GdCu_2O_8$ for $x = 0$, 0.01, 0.03, 0.05, 0.075 and 0.10 as obtained by Rietveld refinements of powder X-ray diffraction patterns recorded at room temperature employing the tetragonal space group *P4/mmm*

x	0	0.01	0.03	0.05	0.075	0.10
a (Å)	3.8399(2)	3.8378(2)	3.8373(2)	3.8387(2)	3.8386(1)	3.8435(2)
c (Å)	11.5766(6)	11.5686(7)	11.5683(5)	11.5649(8)	11.5639(3)	11.5603(7)
V (Å^3)	170.7	170.4	170.3	170.4	170.4	170.8
z(Sr)	0.3108(7)	0.3091(6)	0.3121(5)	0.3097(7)	0.3122(5)	0.3136(5)
z(Cu)	0.1484(9)	0.1499(9)	0.1496(8)	0.1520(10)	0.1490(9)	0.1505(9)
x(O_1)	0.041(39)	0.014(14)	0.051(60)	0.035(40)	0.002(20)	0.030(40)
z(O_1)	0.338(3)	0.329(3)	0.337(3)	0.330(4)	0.334(3)	0.333(4)
z(O_2)	0.123(2)	0.123(2)	0.124(2)	0.120(2)	0.129(2)	0.119(2)
x(O_3)	0.117(12)	0.120(12)	0.130(10)	0.114(15)	0.139(11)	0.141(13)
ϕ(Ru–O–Cu)	171(4)	176(4)	169(4)	172(4)	179(4)	173(4)
Ti Con. (%)	0 (fix)	1 (fix)	3.5(5)	5.8(5)	8.9(5)	9.5(5)
R_{Bragg} (%)	5.86	4.78	5.8	7.46	4.98	7.48

Listed are the lattice constants a ($=b$) and c, the unit-cell volume V, the positional parameters (for atoms with refinable position parameters only), the angle ϕ of the Cu–O–Ru bond, the Ti concentration as determined from refined occupancy values, and the Bragg reliability factors R_{Bragg} of the crystallographic structures.

Table 2
Crystallographic properties of $Ru_{1-x}Rh_xSr_2GdCu_2O_8$ for $x = 0$, 0.05, 0.075, 0.1, 0.15 and 0.2 as obtained by Rietveld refinements employing the tetragonal space group *P4/mmm*

x	0	0.05	0.075	0.1	0.15	0.2
a (Å)	3.8399(2)	3.8375(1)	3.8362(1)	3.8374(1)	3.8367(1)	3.8368(2)
c (Å)	11.5766(6)	11.5709(6)	11.5653(6)	11.5643(3)	11.5649(5)	11.5559(9)
V (Å^3)	170.7	170.4	170.2	170.3	170.2	170.1
z(Sr)	0.3108(7)	0.3096(6)	0.3113(6)	0.3102(5)	0.3312(6)	0.3113(9)
z(Cu)	0.1484(9)	0.1488(9)	0.1475(9)	0.1429(8)	0.1463(9)	0.1472(14)
x(O_1)	0.041(39)	0.019(48)	0.014(72)	0.015(54)	0.054(62)	0.047(44)
z(O_1)	0.338(3)	0.331(3)	0.333(3)	0.333(3)	0.333(3)	0.335(6)
z(O_2)	0.123(2)	0.123(2)	0.127(2)	0.125(2)	0.127(2)	0.125(3)
x(O_3)	0.117(12)	0.120(12)	0.135(14)	0.140(11)	0.129(11)	0.125(24)
ϕ(Ru–O–Cu)	171(4)	176(4)	177(4)	176(4)	168(4)	170(4)
Rh Con. (%)	0 (fix)	5 (fix)	7.5 (fix)	10 (fix)	15 (fix)	20 (fix)
R_{Bragg} (%)	5.86	7.51	6.83	5.45	7.91	8.65

Listed are the lattice constants a ($=b$) and c, the unit-cell volume V, the positional parameters (for atoms with refinable position parameters only), the angle ϕ of the Cu–O–Ru bond, and the Bragg reliability factors R_{Bragg} of the crystallographic structures. Due to the small difference of only one electron between Ru and Rh the measurements did not allow for a refinement of the doping concentration.

respectively. The resistivity of the pure sample decreases with decreasing temperature, passes through a shallow minimum at $T = 87$ K and then slowly increases before the onset of superconductivity at $T_c = 50$ K. Asimilar behavior is observed for all superconducting Ti- and Rh-doped samples. The shallow minimum is shifted to higher temperatures for increasing x. The highest doped samples $x = 0.1$ (Ti) and $x = 0.2$ (Rh) show a semiconducting behavior.

The resistivity of the 10% Ti-doped sample is shown in the inset of Fig. 2 for the full temperature range. It is obvious from the inset that the resistivity always increases with decreasing temperatures. Malo et al. [29] show a negative, diamagnetic signal in the ac magnetic susceptibility at a stimulus of $H_{ac} = 0.01$ Oe and a frequency $v = 133$ Hz for 10% Ti. We did not observe any traces of superconductivity in the resistivity, and either in the zero field cooled (ZFC) susceptibility

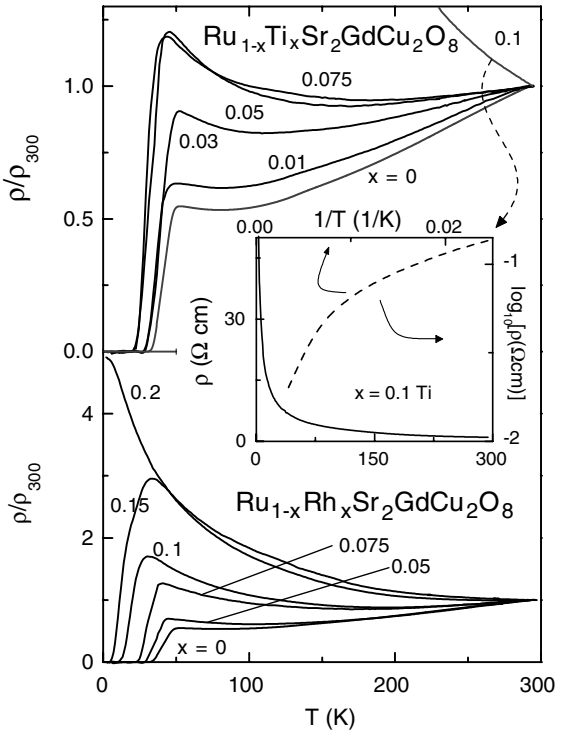

Fig. 2. Normalized electrical resistivities vs. temperatures for Ti (upper frame) and Rh (lower frame) doped compounds (including undoped material). The inset displays the data for the insulating $Ru_{0.9}Ti_{0.1}Sr_2GdCu_2O_8$ in linear ($\rho(T)$) and Arrhenius-type ($\log_{10}\rho(1/T)$) representation.

for this sample. These different results may be attributed to the different preparation routes which play an important role for the superconducting and magnetic properties of Ru-1212 [39–41]. Nevertheless, it is remarkable that in our case already 10% Ti-doping leads to a completely insulating behavior which demonstrates the closeness of Ru-1212 to a metal-to-insulator transition (MIT).

All compounds reveal a non-linear temperature dependence for $T > T_c$ unlike other high-T_c superconductors (HTSC) [38]. In the literature deviations from a linear resistivity behavior are sometimes discussed within the context of a normal-state pseudo-gap for underdoped samples [28]. In our case the polycrystalline character of the samples prevents a detailed analysis of such features, as the anisotropic transport properties of the *c*-axis and the *ab*-plane, respectively, cannot be separated. Moreover, a significant contribution of defects to the electrical transport or a segregation into insulating phases at the grain boundaries cannot be excluded in the present case of ceramic samples. Such a defect dominated transport may also account for deviations from a purely thermally activated conductivity, as it is evidenced by an Arrhenius-type representation of the resistivity in the inset of Fig. 2. On the other hand, the doping phase diagram of $Y_{1-x}Ca_xBa_2(Cu_{1-y}Zn_y)_3O_{7-\delta}$ has recently been investigated by transport measurements employing polycrystalline samples [42]. The results were relatively insensitive of doping concentration and crystalline state, as good agreement has been found to previously published resistivity data of single crystals [42]. Furthermore, optical spectroscopy of $RuSr_2GdCu_2O_8$ showed a suppression of the optical conductivity spectral weight at low frequencies below a characteristic temperature of $T^* = 90$ K [21]. Though more pronounced in other high-T_c superconducting compounds, this characteristic behavior is consistent with the opening of a normal state pseudo-gap in Ru-1212 [21]. Though we have to critically consider the above mentioned difficulties in interpreting resistivity data from ceramic samples, the present transport data seem to be consistent with the scenario of a normal state pseudo-gap in doped Ru-1212, as found in other high-T_c materials [11,42].

For all investigated samples, an upturn of the resistivity just above T_c can be detected on decreasing temperature and the corresponding minimum, which separates $\partial\rho/\partial T > 0$ from $\partial\rho/\partial T < 0$ is shifted towards higher temperatures for higher doping. Similar features of the resistivity as found for the presently investigated Ru-1212 systems were observed also for $Ru(Sr_{1-x}La_x)_2GdCu_2O_8$ [33]. In principle, the substitution of Ti^{4+} and Rh^{3+} for mixed valent Ru^{4+}/Ru^{5+} is expected to increase T_c with increasing x due to the increase of the hole concentration towards optimal doping. This is different from electron dopants like La^{3+} substituted for Sr^{2+} or Ce^{4+} substituted for Gd^{3+}, where the superconductivity is suppressed rather fast due to the reduction of the charge carrier density [25,33]. We speculate that the main reason for the decrease of T_c under doping of Rh or Ti is the

atomic disorder induced by the dopants. Defect assisted trapping may thus lead to an effective reduction of the charge carrier density. The influence of disorder on the mobility edge is especially important due to the low carrier density and the closeness of a MIT even in pure Ru-1212.

3.3. DC magnetic properties

DC magnetic susceptibilities of the pure and doped compounds were measured in an applied magnetic field of 1 kOe. Fig. 3 represents the temperature dependence of the DC magnetic susceptibility χ of the Ti (upper frame) and Rh (lower frame) doped compounds. The insets show the inverse magnetic susceptibility $1/\chi$ of all Ti samples and of the Rh sample with $x = 0.15$. It is worthwhile to note that the substitution of Ru by Ti or Rh leads to a dilution of the magnetic RuO_2 layers and the magnetic ordering temperatures shift to lower temperatures on increasing x. The lowering of the magnetic ordering temperature is accompanied by a continuous decrease of the ferromagnetic magnetization for increasing doping concentration. The substitutional cations probably break the Ru–O–Ru antiferromagnetic interaction paths resulting in a decrease of T_N. Due to the nonmagnetic electronic configuration of both Rh^{3+} and Ti^{4+}, T_N changes similarly in the two substitutional series. We attempted to fit the inverse magnetic susceptibility by using two independent Curie–Weiss contributions to calculate the effective paramagnetic moment of Ru ions, as well as to get an estimate of the ordering temperature of all doped compounds. The magnetic parameters of Gd ions were fixed [33] at an effective paramagnetic moment $\mu_{eff} = 7.94\ \mu_B$ and a Curie–Weiss constant $\Theta = -4$ K. Arepresentative fit is shown in the lower inset of Fig. 3. The fitting parameters of the Ti- and Rh-doped compounds are given in Table 3. For both doping series the paramagnetic moment is slightly increasing, but is always close to a value of 2.8 characteristic for a spin $S = 1$ system. One would expect that the moment

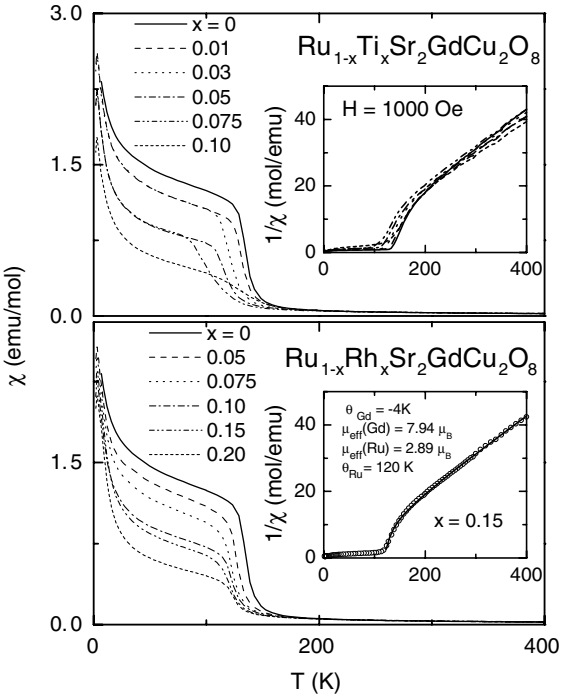

Fig. 3. The temperature dependence of the DC susceptibilities (χ) of Ru-1212 (upper frame for Ti and lower one for Rh-doped compounds). The inset of the upper frame shows the inverse DC magnetic susceptibilities $1/\chi$ vs. temperature (2–400 K) for all investigated Ti samples, while the inset in the lower frame shows exemplarily the fitting employing two independent Curie–Weiss fitting contributions for $x = 0.15$ Rh.

Table 3
Magnetic properties of $Ru_{1-x}Ti_xSr_2GdCu_2O_8$ (upper frame) and $Ru_{1-x}Rh_xSr_2GdCu_2O_8$ (lower frame)

x(Ti)	0	0.01	0.03	0.05	0.07	0.10
μ_{eff} (μ_B)	2.89(23)	3.08(32)	2.86(29)	3.08(38)	2.75(29)	3.31(19)
θ (K)	134.0(4)	131.0(5)	127.0(4)	118.0(8)	116.0(5)	127.0(13)
x(Rh)	0	0.05	0.075	0.10	0.15	0.20
μ_{eff} (μ_B)	2.89(23)	2.99(30)	3.03(35)	3.48(51)	2.89(24)	3.14(37)
θ (K)	134.0(4)	130.0(4)	125.0(6)	117.1(4)	120.0(4)	116.0(9)

The parameters were obtained by fitting $\chi^{-1}(T)$ data, as shown in the inset of Fig. 3, employing two independent Curie–Weiss contributions from Ru and Gd sublattices, respectively. The parameters of Gd ions; $\mu_{eff} = 7.94\ \mu_B$ and $\Theta = -4$ K were kept fixed.

becomes slightly reduced when doping 10% (Ti) or 20% (Rh) non-magnetic ($S = 0$) impurities. This is not observed. However, the Curie–Weiss temperature becomes reduced which indeed is expected.

The temperature dependencies of zero field cooling (ZFC) and field cooling (FC) branches as measured in an external field of $H = 5$ Oe are shown in Fig. 4 for all compounds investigated. At T_N there is a clear splitting of FC and ZFC susceptibilities. All superconducting compounds exhibit a diamagnetic signal in the ZFC branches at temperatures significantly smaller than T_c as determined from the resistivity measurements. This behavior is attributed to the reduction of H_{c1} due to impurity scattering or grain-size effects within the polycrystalline ceramic samples [12]. Most of the doped samples show also a diamagnetic contribution in FC magnetization curves but there is no evidence for a complete MS due to the presence of a spontaneous vortex phase (SVP) [12,20].

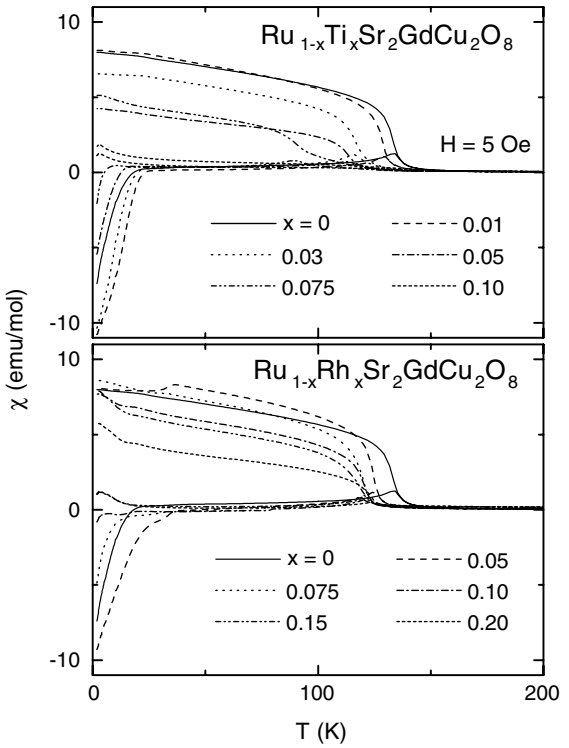

Fig. 4. Field cooling (FC) and zero field cooling (ZFC) branches for all Ti (upper frame) and Rh (lower frame) compounds (including the undoped compound) in an external field of $H = 5$ Oe.

3.4. Phase diagram

Finally, Fig. 5 shows the (x, T)-phase diagram for the doped Ru-1212 system including our previous results on La-doped samples [33]. The superconducting transition temperature was determined as the mid-point [43] of the resistivity decrease towards zero resistance (Fig. 2). It is clear that T_N and T_c depend on the substitutional cation and on the element for which it is substituted. For La^{3+} doping, superconductivity appears only in a narrow doping range ($x \leqslant 0.03$), while the magnetic ordering temperature is enhanced with increasing x. On the other hand, substituting Ru by Ti^{4+} ($3d^0$) or Rh^{3+} ($4d^6$) reduces the magnetic ordering temperature of RuO_2 layers but SC survives for a considerable range of doping concentrations ($x \leqslant 0.075$ for Ti and $x \leqslant 0.15$ for Rh). It becomes clear from Fig. 5 that 10% Ti suppresses superconductivity, while for the same effect 20% Rh is needed. It also seems that magnetic order is stronger influenced by Ti than by Rh doping.

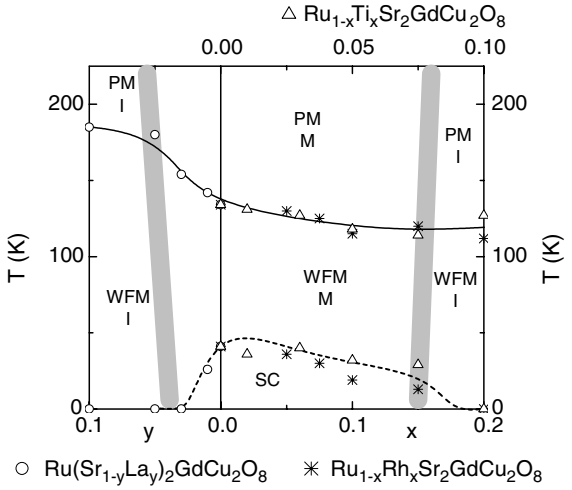

Fig. 5. Generalized phase diagram of the Ru-1212 system. Plotted is transition temperature vs. doping concentration for different dopants. The doping parameter y (from zero to the left) denotes a decrease of the hole concentration in the system $Ru(Sr_{1-y}La_y)_2GdCu_2O_8$. The doping parameter x corresponds to an increase of the charge carrier density in the systems $Ru_{1-x}M_xSr_2GdCu_2O_8$ with M = Ti (upper scale, $0 \leqslant x \leqslant 0.1$) and Rh (lower scale, $0 \leqslant x \leqslant 0.2$). The shaded areas represent the crossover regions from insulating to metallic behavior as evaluated from $\partial\rho/\partial T$ for temperatures well above T_c.

Above T_c up to the magnetic ordering temperature, a weak ferromagnetic metallic (WFM) phase is observed. Close to the critical concentration, where the superconductivity becomes suppressed, a weak ferromagnetic insulator (WFI) shows up. Furthermore, the system is a paramagnetic metal (PM) at temperatures above the magnetic ordering temperatures of the superconducting samples but becomes a paramagnetic insulator (PI) at the critical concentration and low temperatures. For typical underdoped high-T_c superconductors, the superconducting transition temperature $T_c \approx 45$ K corresponds to a charge carrier concentration of approximately 0.1 holes per Cu ion [26]. The rare earth ions are expected to be trivalent, whereas, as usual, the SrO layers are assumed to be charge neutral. Then charge balance implies a mixed valency of Ru ions, as observed experimentally [15–17], with 20% Ru^{4+} and 80% Ru^{5+} ions. It is obvious that superconductivity is strongly affected by La doping. La^{3+} substitutes Sr^{2+} and reduces the hole concentration in the CuO_2 planes [33]. Rh^{3+} and Ti^{4+} increase hole doping and one would expect that T_c increases. Probably due to disorder and localization effects this is not the fact. However, in case of hole doping superconductivity survives much longer than in case of electron doping and for Rh^{3+} superconductivity still can be observed for doping levels $x = 0.15$.

4. Conclusions

We have presented a detailed investigation of structural, electronic and magnetic properties of Ti- and Rh-doped Ru-1212 compounds. There is no significant change of the lattice parameters or of the Ru–O–Ru bond angle ϕ within the concentration range investigated. The results were compared with La-doped compounds and a phase diagram for Ru-1212 system is constructed. The relation between superconductivity and ferromagnetism in this system is still not fully understood, but the RuO_2 layers play an important role, as well as the bond angle ϕ of Ru–O–Cu and the bond length of Cu–O.

Both, Ti and Rh dopants reduce the ferromagnetism and the superconductivity but at a different rate due to the difference of their electronic configuration. These results are consistent with Nb-doped compounds as reported earlier [34]. Despite the fact that the hole concentration is increased, the superconducting transition temperature decreases for both dopants, most probably due to disorder that prevents charge delocalization between adjacent RuO_2 and CuO_2 layers.

Even without considering superconductivity, it should be emphasized that the magnetic properties of Ru-1212 themselves are rather unusual. Magnetic measurements show typical features of a ferromagnetic system (in particular an abrupt increase of the magnetization in small external fields, as well as a positive Curie temperature) despite an overall antiferromagnetic structure, as determined by neutron diffraction [10]. Alternatively to a static spin canting producing a ferromagnetic component, the magnetism of Ru-1212 has also been analyzed in terms of double exchange [19].

The electronic structure of Ru-1212 is then composed of antiferromagnetically arranged localized spins at each Ru site (corresponding to Ru^{5+}) and additional itinerant electrons (representing Ru^{4+}). Within the double exchange model, the itinerant electrons are ferromagnetically coupled to the localized spins. The ferromagnetic properties can now be accounted for by the formation of ferromagnetic polarons [19]. In this model double exchange would strongly be suppressed when doping non-magnetic impurities and this really has been observed when doping Rh or Ti for Ru.

Concluding, it seems clear that in Ru-1212 a much smaller doping range is accessible as compared to the R123 high-T_c compounds where the oxygen content can easily be tuned from O_6 to O_7. This narrow doping range probably results from the existence of many neighboring stable phases.

Acknowledgements

This work was partly supported by Bundesminterium fur Bildung und Forschung (BMBF) via VDI/EKM 13N6917/18 and by the DFG within SFB 484 (Augsburg).

References

[1] A. Felner, U. Asaf, Y. Levi, O. Millo, Phys. Rev. B 55 (1997) 3374.
[2] E.B. Sonin, I. Felner, Phys. Rev. B 57 (1998) 14000.
[3] J. Tallon, C. Bernhard, M. Bowden, P. Gilberd, T. Stoto, D. Pringle, IEEE. Trans. Appl. Supercond. 9 (2) (1999) 1696.
[4] A.C. McLaughlin, W. Zhou, J.P. Attfield, A.N. Fitch, J.L. Tallon, Phys. Rev. B 60 (1999) 7512.
[5] C. Bernhard, J.L. Tallon, Ch. Neidermayer, Th. Blasius, A. Golnik, E. Brucher, P.K. Kremer, R. Noakes, C.E. Stronach, E.J. Ansaldo, Phys. Rev. B 59 (1999) 14099.
[6] O. Chmaissem, J.D. Jorgensen, H. Shaked, P. Dollar, J.L. Tallon, Phys. Rev. B 61 (2000) 6401.
[7] W.E. Pickett, R. Weht, A.B. Shick, Phys. Rev. Lett. 83 (1999) 3713.
[8] I. Matsburara, N. Kido, R. Funahashi, J. Phys. Condens. Matter 13 (2001) 5645.
[9] J.D. Jorgensen, O. Chmaissem, H. Shaked, S. Short, P.W. Klamut, B. Dabrowski, J.L. Tallon, Phys. Rev. B 63 (2001) 54440.
[10] J.W. Lynn, B. Keimer, C. Urlich, C. Bernhard, J.L. Tallon, Phys. Rev. B 61 (2000) 14964.
[11] V.M. Williams, S. Krämer, Phys. Rev. B 62 (2000) 4132.
[12] C. Bernhard, J.L. Tallon, E. Brucher, R.K. Kremer, Phys. Rev. B 61 (2000) 14960.
[13] L. Bauerfeind, W. Widder, H.F. Braun, Physica C 254 (1995) 151.
[14] L. Bauerfeind, W. Widder, H.F. Braun, J. Low Temp. Phys. 105 (1996) 1605.
[15] A. Butera, A. Fainstein, E. Winkler, J. Tallon, Phys. Rev. B 63 (2001) 54442.
[16] K. Kumagai, S. Takada, Y. Furukawa, Phys. Rev. B 63 (2001) 180509.
[17] R.S. Liu, L.-Y. Jang, H.-H. Hung, J.L. Tallon, Phys. Rev. B 63 (2001) 212507.
[18] J. Hemberger, A. Krimmel, T. Kurz, H.-A. Krug von Nidda, V.Yu. Ivanov, A.A. Mukhin, A.M. Balbashov, A. Loidl, Phys. Rev. B 66 (2002) 094410.
[19] H. Aliaga, A.A. Aligia, Physica B 320 (2002) 34.
[20] Y. Tokunaga, H. Kotegawa, K. Ishida, Y. Kitaoka, H. Takagiwa, J. Akimitsu, Phys. Rev. Lett. 86 (2001) 5767.
[21] A.V. Boris, P. Mandal, C. Bernhard, N.N. Kovaleva, K. Pucher, J. Hemberger, A. Loidl, Phys. Rev. B 63 (2001) 184505.
[22] P.W. Klamut, B. Dabrowski, S. Kolesnik, M. Maxwell, J. Mais, Phys. Rev. B 63 (2001) 224512.
[23] C.W. Chu, Y.Y. Xue, S. Tsui, J. Cmaidalka, A.K. Heilman, B. Lorenz, R.L. Meng, Physica C 335 (2000) 231.
[24] Y.Y. Xue, R.L. Meng, J. Cmaidalka, B. Lorenz, L.M. Desaneti, A.K. Heilman, C.W. Chu, Physica C 341–348 (2000) 459.
[25] P.W. Klamut, B. Dabrowski, J. Mais, M. Maxwell, Physica C 350 (2001) 24.
[26] A.C. McLaughlin, J.P. Attfield, Phys. Rev. B 60 (1999) 14605.
[27] J.T. Rijssenbeek, N. Mansourian-Hadavi, S. Malo, D. Ko, C. Washburn, A. Maignan, D. Pelloquin, T.O. Mason, K.R. Poppelmeier, Physica C 341–348 (2000) 481.
[28] J.L. Tallon, J.W. Loram, Physica C 349 (2001) 53.
[29] S. Malo, D. Ko, J.T. Rijssenbeek, A. Maignan, D. Pelloquin, V.P. Dravid, K.R. Poeppelmeier, J. Inorg. Mater. 2 (2000) 601.
[30] J.L. Tallon, J.W. Loram, G.V.M. Williams, C. Bernhard, Phys. Rev. B 61 (2001) R6471.
[31] B. Nachumi, A. Keren, K. Kojima, M. Larkin, G.M. Luke, J. Merrin, O. Tchernyshöv, Y.J. Uemura, N. Ichikawa, M. Goto, S. Uchida, Phys. Rev. Lett. 77 (1996) 5421.
[32] Y. Fukuzumi, K. Mizuhashi, K. Takenaka, S. Uchida, Phys. Rev. Lett. 76 (1996) 684.
[33] P. Mandal, A. Hassen, J. Hemberger, A. Krimmel, A. Loidl, Phys. Rev. B 64 (2002) 144506.
[34] A.C. McLaughlin, V. Janowitz, J.A. McAllister, J.P. Attfield, J. Mater. Chem. 11 (2001) 173.
[35] P.W. Klamut et al., in: Ruthenate and Rutheno-Cuprate Materials, Unconventional Superconductivity, Magnetism and Quantum Phase Transitions, Lecture Notes in Physics, vol. 603, Springer-Verlag, 2002.
[36] M. Hrovat, A. Bencan, Z. Samardzija, J. Holc, A. Brglez, D. Mihailovic, J. Mater. Sci. Lett. 19 (2000) 919.
[37] M. Hrovat, A. Bencan, J. Holc, Z. Samardzija, D. Mihailovic, J. Mater. Sci. Lett. 19 (2000) 1423.
[38] D.M. Ginsberg, Physical Properties of High Temperature Superconductors III, World Scientific, London, 1992.
[39] I. Felner, U. Asaf, S. Reich, Y. Tsabba, Physica C 311 (1999) 163.
[40] C. Artini, M.M. Carnasciali, G.A. Costa, M. Ferretti, M.R. Cimberle, M. Putti, R. Masini, Physica C 377 (2002) 431.
[41] T. Papageorgiou, T. Herrmannsdörfer, R. Dinnebier, T. Mai, T. Ernst, M. Wunschel, H.F. Braun, Physica C 377 (2002) 383.
[42] S.H. Naqib, J.R. Cooper, J.L. Tallon, cond-mat/0301375, 2003.
[43] S. Murase, K. Itoh, H. Wada, K. Noto, Y. Kimura, Y. Tanaka, K. Osamura, Physica C 357–360 (2001) 1197.